BNL-111844-2016-JA

PERSPECTIVE

Catalytic reduction of CO_2 by H_2 for synthesis of CO, methanol and hydrocarbons: Challenges and opportunities

Received 00th January 20xx,
Accepted 00th January 20xx

DOI: 10.1039/x0xx00000x

Marc D. Porosoff,[a] Binghang Yan[b] and Jingguang G. Chen[b]

Ocean acidification and climate change are expected to be two of the most difficult scientific challenges of the 21st century. Converting CO_2 into valuable chemicals and fuels is one of the most practical routes for reducing CO_2 emissions while fossil fuels continue to dominate the energy sector. Reducing CO_2 by H_2 using heterogeneous catalysis has been studied extensively, but there are still significant challenges in developing active, selective and stable catalysts suitable for large-scale commercialization. The catalytic reduction of CO_2 by H_2 can lead to the formation of three types of products: CO through the reverse water-gas shift (RWGS) reaction, methanol via selective hydrogenation, and hydrocarbons through combination of CO_2 reduction with Fischer-Tropsch (FT) reactions. Investigations into these routes reveal that the stabilization of key reaction intermediates is critically important for controlling catalytic selectivity. Furthermore, viability of these processes is contingent on the development of a CO_2-free H_2 source on a large enough scale to significantly reduce CO_2 emissions.

Introduction

A As atmospheric concentrations of CO_2 continue to rise, efforts must be put forth to avoid negative effects of climate change and ocean acidification.[1, 2] Stabilization of atmospheric CO_2 levels requires both significant cuts in emissions and active removal of CO_2 from the atmosphere.[3] Utilizing CO_2 in a catalytic process to manufacture valuable chemicals and fuels is more desirable than sequestration[4, 5] because the net amount of CO_2 mitigated by conversion with renewable energy is 20 – 40 times greater than sequestration over a 20 year span.[6] Additionally, the products of CO_2 conversion are value-added and can be used as fuels or precursors to produce more complex chemicals and fuels.

To substantially reduce CO_2 emissions by catalytic conversion, only reactions which produce fuels or commodity chemicals can be considered as viable solutions. The demand for fine chemicals is simply not large enough to effectively reduce emissions through a CO_2 conversion process.[7] For example, assuming all fuels and chemicals would be produced using CO_2 as the feedstock, demand for organic chemicals only accounts for 4% of CO_2 emissions, while fuels account for 30% of total CO_2 emissions and 100% of emissions from power plants.[8] Therefore, conversion to fuels represents a greater impact than to specialty chemicals for achieving a substantial CO_2 reduction.

Current efforts into CO_2 reduction focus on the development of highly active, selective and stable catalysts in two categories, electrochemical and thermal reduction of CO_2. Electrochemical reduction of CO_2 would most likely operate on a smaller scale and is more desirable for localized CO_2 conversion and production of fine chemicals. There are extensive reports regarding electrochemical CO_2 reduction, but they are outside the scope of this perspective and can be found elsewhere.[9, 10] Research into catalysts for the thermal reduction of CO_2 can be further divided into the production of three classes of products, CO, methanol (MeOH) and hydrocarbons.

CO produced by reverse water-gas shift (RWGS) offers high flexibility because CO can be used in both MeOH synthesis and downstream Fischer-Tropsch (FT) for chemicals and fuels. However, RWGS is an endothermic process, which requires high temperatures and the conversion is equilibrium limited to ~23% at 300 °C and 1 MPa.[11] Because the maximum conversion of CO_2 ranges from 10% to 50% from 200 °C to 500 °C with a 3:1 H_2:CO_2 ratio, efforts must be put forth to develop active catalysts to overcome the slow kinetics and ensure CO is produced at the maximum allowable yield.

CO_2 conversion to MeOH is the most direct route for CO_2 utilization because MeOH can be used as a fuel additive, fuel substitute and precursor to many commodity chemicals.[12] Although MeOH synthesis from CO_2 and H_2 is exothermic, CO_2 conversion to MeOH is kinetically limited at low temperatures and thermodynamically limited at high temperatures, resulting in a low theoretical MeOH yield of 0.06% at 300 °C and 0.1 MPa.[13] In typical industrial MeOH synthesis, CO, H_2 and a small amount of CO_2 are reacted over a $Cu/ZnO/Al_2O_3$ catalyst between 5 – 10 MPa at 220 – 300 °C.[14] $Cu/ZnO/Al_2O_3$ has also been investigated for MeOH synthesis from CO_2 and H_2, but

[a] Department of Chemical Engineering, Columbia University, 500 W. 120th Street, New York, NY 10027 (USA).
[b] Chemistry Department, Brookhaven National Laboratory, 2 Center Street, Upton, NY 11973 (USA).

† Footnotes relating to the title and/or authors should appear here.
Electronic Supplementary Information (ESI) available: [details of any supplementary information available should be included here]. See DOI: 10.1039/x0xx00000x

further improvements are needed to improve MeOH selectivity and yield.

Direct hydrogenation of CO_2 can also lead to the production of hydrocarbons, including both alkanes and olefins. Direct hydrogenation of CO_2 to $–CH_2–$ species is possible through dissociative adsorption followed by hydrogenation, but the extent to which this occurs is not well known.[11] Another possible route is direct FT from CO_2 and H_2 (CO_2-FT) by performing RWGS followed by FT in one reactor, which is thermodynamically easier than RWGS because the overall process is exothermic.[15] The CO_2-FT process is very attractive because it provides a route to directly produce alkanes and olefins from CO_2 and H_2, but designing catalysts that are water resistant with high olefin selectivity is challenging. Out of the three CO_2 conversion processes mentioned, CO_2 hydrogenation to long-chain hydrocarbons is the least studied and characterized process.

In this perspective, each of the three pathways of CO_2 reduction by H_2 will be reviewed in the order of (1) CO_2 to CO via the RWGS reaction over bimetallic and carbide catalysts, (2) CO_2 to MeOH over Cu-based catalysts and other materials and (3) CO_2 to hydrocarbons via CO_2-FT over redesigned FT catalysts. The perspective will conclude by discussing challenges and opportunities for further advancing the field of CO_2 reduction by H_2.

CO Production through Reverse Water-Gas Shift

Typical RWGS catalysts consist of well isolated and dispersed nanoparticles supported on a metal-oxide to maximize the interfacial area between the metal and the support.[16] The interfacial region is important because both the metal and support are involved in the RWGS chemistry. Two reaction pathways have been proposed for CO formation from RWGS. One is the redox mechanism, where over Cu-based catalysts, CO_2 oxidizes Cu^0 to generate CO and Cu^+ while H_2 reduces Cu^+ to form H_2O.[17] Further evidence for this mechanism is provided by FTIR spectroscopy studies over a Cu/ZnO catalyst which indicate CO_2 dissociates to CO,[18] but formate has also been detected over Cu^0.[19]

The other widely accepted pathway is the formate decomposition mechanism in which CO_2 is first hydrogenated into formate,[20] followed by cleavage of the C=O bond. Therefore, an effective RWGS catalyst should be dual functional with high activity for both hydrogenation and C=O bond scission. Metal nanoparticles supported on metal-oxides are popular materials because dispersed metal catalytic sites dissociate hydrogen relatively easily,[21] which then allows reactive atomic hydrogen to spill-over onto the support and hydrogenate CO_2 that is adsorbed on the oxides.[22]

Based on the proposed mechanisms, an active and selective catalyst for RWGS should consist of both an active metal and metal-oxide support that participate in the reaction steps. Cu-based catalysts, noble metals and catalysts supported on CeO_2 have been studied extensively.[4, 5] Pt-based catalysts are generally popular because of their high hydrogenation activity, with Pt-Co bimetallics showing higher CO production than their parent metals.[23] A detailed study into Pt-Co supported on MCF-17 with ambient pressure X-ray photoelectron spectroscopy (AP-XPS) and environmental transmission electron microscopy (eTEM) reveals that the surface is enriched in Pt, explaining the Pt-like selectivity of Pt-Co. In comparison with the pure Co catalyst, the addition of Pt aids the reduction of Co, shifting the selectivity primarily toward CO.[24] Details of the activity and selectivity with reaction conditions of several representative RWGS catalysts are compared in Table 1.

Although Pt-based catalysts are active and selective for RWGS, their high cost is unattractive for large scale conversion of CO_2. Fe-based catalysts are promising and show high activity and selectivity for RWGS,[25] while a bimetallic Fe-Mo catalyst has a decreased particle size with higher Fe dispersion and improved stability from the formation of a $Fe_2(MoO_4)_3$ phase.[26] Bimetallic Ni-Mo shows similar behavior to the Fe-Mo system[27] and NiO supported on mesporous CeO_2 shows high CO selectivity when the NiO particles are well dispersed on the support.[16]

While the metallic phase is clearly important for RWGS selectivity, the reducibility of the metal-oxide support can significantly influence the activity. CeO_2 is a common support for RWGS because of its reducibility and high intrinsic activity toward CO_2 adsorption. DFT studies indicate that the CeO_2(110) surface is more catalytically active than (100) or (111), likely because the creation of oxygen vacancies is most facile on CeO_2(110).[28] For Pt nanoparticles supported on CeO_2, temporal analysis of products (TAP) studies with isotopically labeled CO_2 indicate that the order of H_2 and CO_2 adsorption on the surface is critical. The presence of Pt improves oxygen exchange of CO_2 with oxygen defects in CeO_2.[29] The addition of CeO_2 to catalysts supported on irreducible oxides can also improve activity, as Pd/CeO_2-γ-Al_2O_3 is more active than Pd/γ-Al_2O_3 because of the ability of CeO_2 to exchange oxygen.[30]

CeO_2 is clearly a well-studied reducible support for RWGS, but other reducible metal-oxides are also promising. CO_2 binds on In_2O_3 in a bent configuration and has an exothermic energy of adsorption, which contributes to the high activity.[31] Ga_2O_3 is an active support and can be further improved by the addition of CeO_2, which enhances the generation of bicarbonate intermediates that readily dissociate into CO and H_2O.[32] TiO_2 is another reducible support that is active for RWGS and it has been shown that Pt/TiO_2 outperforms the irreducible Pt/γ-Al_2O_3 catalyst.[33]

Table 1. Summary of reaction conditions with conversion and selectivity to CO, when available, for selected RWGS catalysts.

Catalyst	H_2:CO_2 Ratio	Temperature (°C)	Pressure (MPa)	Conversion (%)	Selectivity (%)
NiO/CeO_2[16]	1:1	700	0.1	~40	~100
Cu/Al_2O_3[20]	1:9	500	N/A	~60	N/A
Co/MCF-17[24]	3:1	200 – 300	0.55	~5	~90
Pt-Co/MCF-17[24]	3:1	200 – 300	0.55	~5	~99
Cu/SiO_2[34]	1:1	600	0.1	5.3	N/A
$Cu/K/SiO_2$[34]	1:1	600	0.1	12.8	N/A
$Cu\text{-}Ni/\gamma\text{-}Al_2O_3$[35]	1:1	600	0.1	28.7	79.7
$Cu\text{-}Fe/SiO_2$[36]	1:1	600	0.1	15	N/A
Li/RhY[37]	3:1	250	3	13.1	86.6
Rh/SiO_2[38]	3:1	200	5	0.52	88.1
Rh/TiO_2[25]	1:1	270	2	7.9	14.5
Fe/TiO_2[25]	1:1	270	2	2.7	73.0
$Rh\text{-}Fe/TiO_2$[25]	1:1	270	2	9.2	28.4
$Fe\text{-}Mo/\gamma\text{-}Al_2O_3$[26]	1:1	600	1	~45	~100
$Mo/\gamma\text{-}Al_2O_3$[27]	1:1	600	1	34.2	97
Pd/Al_2O_3[30]	1:1	260	0.1	N/A	78
$Pd/CeO_2/Al_2O_3$[30]	1:1	260	0.1	N/A	87
$Pd/La_2O_3/Al_2O_3$[30]	1:1	260	0.1	N/A	70
$CeO_2\text{-}Ga_2O_3$[32]	1:1	500	0.1	11.0	N/A
Pt/TiO_2[33]	1.4:1	400	N/A	~30	N/A
Pt/Al_2O_3[33]	1.4:1	400	N/A	~20	N/A
$PtCo/CeO_2$[39]	3:1	300	0.1	3.3	71.0
Co/CeO_2[39]	3:1	300	0.1	3.8	39.4
$PtCo/\gamma\text{-}Al_2O_3$[39]	3:1	300	0.1	5.1	89.4
$Co/\gamma\text{-}Al_2O_3$[39]	3:1	300	0.1	3.8	67.0
Mo_2C[39]	3:1	300	0.1	8.7	93.9
Mo_2C[40]	5:1	250	2	17	34
$Cu\text{-}Mo_2C$[40]	5:1	250	2	13	40
$Ni\text{-}Mo_2C$[40]	5:1	250	2	21	29
$Co\text{-}Mo_2C$[40]	5:1	250	2	23	24

The aforementioned combinations of metal and oxide phases require the presence of active and stable interfacial regions for RWGS. In principle, an ideal catalyst should consist of one phase that can perform both hydrogenation and C=O bond scission to selectively produce CO from CO_2. One promising class of catalysts are transition metal carbides (TMCs), which have shown desirable behavior for reactions involving CO_2[41] and properties similar to precious metals for many other reactions.[42] Perhaps the most interesting TMC for RWGS is Mo_2C because of its low cost, dual functionality for H_2 dissociation and C=O bond scission, and potential to behave similarly to reducible oxides, such as CeO_2.[39] As compared in Figure 1, Mo_2C outperforms Pt-based bimetallic catalysts supported on CeO_2 in terms of both activity for CO_2 conversion and selectivity toward CO production.

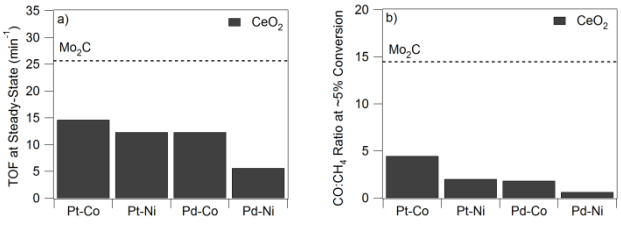

Figure 1. TOF (a) and selectivity (b) at 300 °C on bimetallic supported catalysts on CeO_2 (black bars) and Mo_2C (dashed line). (Reproduced from ref. 39 with permission from John Wiley and Sons.)

Several mechanistic studies have been performed for CO_2 activation over Mo_2C to understand the high intrinsic activity towards CO_2. The findings show that CO_2 binds to Mo_2C in a bent configuration and one of the C=O bonds can spontaneously break,[39, 43] leaving adsorbed CO and O on the catalyst surface. The adsorbed CO can desorb, but the adsorbed O, in the form of an oxycarbide (Mo_2C-O), must be removed by H_2 to complete the catalytic cycle. Because CO_2 activation over TMCs results in oxycarbide formation, the oxygen binding energy (OBE) on the TMC surface is an important descriptor for predicting high RWGS activity.[44] Future studies of CO_2 reduction by H_2 over TMCs should investigate metal-modified carbides as it has been shown that metal can modify the electronic properties of the TMC, thus influencing the OBE and possibly product selectivity.[40]

Methanol Synthesis

Currently the CAMERE (carbon dioxide hydrogenation to form methanol via reverse-water gas shift) process produces MeOH from CO_2 and H_2 at a capacity of ~75 Mt yr^{-1}. The overall process scheme involves RWGS over $ZnAl_2O_4$ followed by water removal and MeOH synthesis over $Cu/ZnO/ZrO_2/Ga_2O_3$, but the disadvantage is that it requires two different catalysts and reactors.[45] An ideal process should use one catalyst in a single reactor, much like current research over $Cu/ZnO/Al_2O_3$, the commercial catalyst for MeOH synthesis from CO and H_2.[46,

[47] This catalyst has shown varying degrees of CO_2 conversion, selectivity and space-time yield, as compared in Table 2 with other catalysts. Although $Cu/ZnO/Al_2O_3$ exhibits promising performance (with a space-time yield up to 7729 g_{MeOH} kg_{cat}^{-1} h^{-1}) under certain conditions (36 MPa and 10:1 H_2:CO_2 ratio),[48] the pressure is likely too high for economic conversion of CO_2.

Table 2. Summary of reaction conditions with conversion, selectivity and space-time yield to MeOH, when available, for selected MeOH synthesis catalysts. Asterisk indicates total alcohol selectivity.

Catalyst	H_2:CO_2 Ratio	Temperature (°C)	Pressure (MPa)	Conversion (%)	Selectivity (%)	Space-Time Yield (g_{MeOH} kg_{cata}^{-1} h^{-1})
$Cu\text{-}ZnO/Al_2O_3$[48]	10:1	260	36	22.7	77.3	7729
$CuO\text{-}ZnO/Al_2O_3$[49]	3.89:1	280	5	19.5	37	311
$CuO\text{-}ZnO/CeO_2$[49]	3.89:1	280	5	12.8	37	210
Cu-Zn-Ga[50]	3:1	270	3	15.9	29.7	135.9
Cu/ZrO_2/CNF[51]	3:1	180	3	14	N/A	34
Cu/plate ZnO/Al_2O_3[52]	2.2:1	270	4.5	10.9	72.7	N/A
$Cu/\gamma\text{-}Al_2O_3$[53]	3.8:1	200	36	8.4	37.3	103.4
$Cu\text{-}K/\gamma\text{-}Al_2O_3$[53]	3.8:1	280	36	28.6	2.1	18.2
$Cu\text{-}Ba/\gamma\text{-}Al_2O_3$[53]	3.8:1	280	10	25.2	9.3	70.7
Pd-CaO/MCM-41[54]	3:1	250	3	12.1	65.2	N/A
Mo_2C[55]	1:3	220	6	4.6	17.7	~21.5
WC[55]	1:3	220	6	1.4	22.4	~8.3
$Cu\text{-}Mo_2C$[55]	1:3	220	6	4	31.5	~33.3
Cu-WC[55]	1:3	220	6	0.6	21.3	~3.4
$Cu\text{-}SiO_2$[55]	1:3	220	6	5.3	34.2	~47.9
$Cu\text{-}ZnO/ZrO_2$[56]	3:1	240	3	17.0	41.5	~48.8
$Cu\text{-}ZnO/TiO_2\text{-}ZrO_2$[56]	3:1	240	3	17.4	43.8	~52.7
$CuO\text{-}ZnO/ZrO_2$[57]	3:1	240	3	18.0	51.2	305
Fe-Cu/MCM-41[58]	3:1	200	1	~2	99.97*	N/A
$Pd\text{-}Cu/SiO_2$[59]	3:1	250	4.1	6.6	34.0	35.7
Pd-Cu/SBA-15[59]	3:1	250	4.1	6.5	23.0	23.0
CoMoS[60]	3:1	310	10.4	28	31	N/A
$Rh\text{-}Sn/SiO_2$[61]	3:1	240	5	2.8	43.1	~23.5
$NiGa/SiO_2$[62]	3:1	160 – 260	0.1	N/A	N/A	90 – 125
$Cu\text{-}ZnO/\gamma\text{-}Al_2O_3$[63]	3:1	250	3	10.1	78.2	76.8
Cu/ZnO[64]	9:1	165	0.1	N/A	61.3	5.2
Cu@ZnO[65] (Core-shell)	3:1	250	3	2.3	100	147.2
La-Mn-Zn-Cu-O[66]	3:1	270	5	13.1	54.5	100
$Cu\text{-}ZnO\text{-}TiO_2$[67]	3:1	220	3	14.8	50.5	51.5
CuO/ZnO[68]	3:1	240	3	16.5	78.2	550
Au/ZrO_2[69]	3:1	240	0.5	9.3	3.4	21.1
Cu/ZrO_2/CNT[70]	3:1	260	3	16.3	43.5	84.0
Pd-ZnO/CNT[71]	3:1	270	5	19.63	35.5	343
Pd/Ga_2O_3[72]	3:1	250	5	17.33	51.62	~175.6
La-Zr-Cu-Zn-O[73]	3:1	250	5	12.6	52.5	100
Cu/Zn/Al/Y[74]	3:1	250	5	26.9	52.4	520
$Ga\text{-}Cu\text{-}ZnO\text{-}ZrO_2$[75]	3:1	250	7	22	72	704
$Cu\text{-}ZnO\text{-}ZrO_2$[76]	3:1	240	5	9.7	62	1200
$La\text{-}Cu/ZrO_2$[77]	3:1	220	3	6.2	66	N/A
Pd-Ga/CNT[78]	3:1	250	5	16.5	52.5	512
$LaCr_{0.5}Cu_{0.5}O_3$[79]	3:1	250	2	10.4	90.8	~278
$Ga_2O_3\text{-}Pd/SiO_2$[80]	3:1	250	3	1.34	58.9	283.4
$Cu/ZnO\text{-}ZrO_2$[81]	3:1	220	8	21	68	181
$Au/ZnO\text{-}ZrO_2$[81]	3:1	220	8	2	100	19
PdO-CuO-ZnO[82]	3:1	240	6	9.19	66.2	322
Cu-Ga/ZnO[83]	3:1	270	2	6.0	88	378
$YBa_2Cu_3O_7$[84]	3:1	240	3	3.4	50.7	N/A

BNL-111844-2016-JA

PERSPECTIVE

Similar to the commercial $Cu/ZnO/Al_2O_3$ catalyst, Cu-based materials are popular choices for MeOH synthesis from CO_2;[49-51] however, activity over Cu-based catalysts is structure sensitive. Ultra-high vacuum (UHV) experiments indicate that Cu(110) is not intrinsically active for CO_2 dissociation,[85] while other studies show Cu(110) is more active toward CO_2 than Cu(111) and Cu(100).[19] To improve interactions with CO_2, many researchers have shown that adding promoters can significantly improve the CO_2 adsorption strength and MeOH selectivity. For example, potassium (K) promoters on Cu/Al_2O_3 stabilize surface intermediates and enhance formate dissociation, lanthanum (La) doping on Cu/ZrO_2 promotes formate hydrogenation to MeOH and inhibits its dissociation into CO,[77] barium (Ba) promoters inhibit formate dissociation and promote MeOH synthesis,[53] and adding CaO to Pd/MCM-41 improves CO_2 adsorption and leads to higher CO_2 conversion and MeOH selectivity.[54] A similar conclusion is obtained over transition metal carbides and those modified with Cu and Au.[55] Cu and Au nanoparticles supported on TiC(001) become charge polarized, which increases CO_2 binding energy, making some of these systems more active than traditional Cu/ZnO catalysts.[86]

The size of the Cu and ZnO crystallites in Cu-ZnO catalysts can also influence the CO_2 adsorption strength on the catalyst,[56] with the catalyst synthesis method playing an important role. CuO/ZrO_2 prepared by deposition-precipitation has a smaller particle size and exhibits higher activity when compared to impregnation or co-precipitation.[87] Catalysts synthesized by the gel-oxalate coprecipitation method show a higher interfacial surface area and MeOH yield than coprecipitation with sodium bicarbonate and complexation with citric acid.[57] On the other hand, a study over Fe-Cu/MCM-41 demonstrates that larger particles with less metal-support interaction are more favorable for CO_2 hydrogenation to alcohols.[58]

In addition to interacting strongly with CO_2, catalysts should stabilize the desired intermediate for high MeOH yield. There are some conflicting studies reporting carboxyl, formic acid or formaldehyde as important intermediates.[88] Other researchers hypothesize that formate is the intermediate over Zn-modified Cu(111),[89, 90] while infrared studies on Cu/SiO_2 contradict the previous study and hypothesize that carboxyl is the intermediate with formate simply acting as a spectator.[91] Furthermore, DFT calculations show that methanol synthesis on Cu(111) is more energetically favorable from hydrocarboxyl (trans-COOH) than formate in the presence of H_2O.[92]

An extensive study combining DFT and UHV experiments on Cu-based model surfaces confirms that stabilization of formyl combined with facile hydrogenation of formate and dioxomethylene (H_2COO) are critical for high MeOH yield.[93] In this case, an ideal catalyst should lower the barrier for H_2COO hydrogenation and exhibit an intermediate CO binding energy. Out of several metals supported on Cu(111), Ni/Cu(111) exhibits the lowest barrier for H_2COO hydrogenation with an intermediate CO binding energy, leading to the highest MeOH production out of Pt, Rh, Pd, Cu and Au supported on Cu(111).[94]

It is well established that Cu is an important metal for promoting MeOH synthesis, but the reducibility of Cu and the nature of the support material can also have a significant effect on the catalytic performance. For example, deactivation over $Cu/ZnO/Al_2O_3$ can be caused by several factors, excess surface hydroxyls, Cu sintering, and decreasing catalyst reducibility from fixation of Cu in the monovalent oxidation state.[95] To improve the catalytic activity and selectivity, Gracini et al. supported a reducible oxide, CeO_x on Cu(111).[96] AP-XPS and infrared reflection absorption spectroscopy (IRRAS) experiments reveal that the metal-oxide Cu-ceria interface directly activates CO_2 in the form of an unstable carboxylate ($CO_2^{\delta-}$), which is a desirable intermediate and opens a new reaction pathway for MeOH synthesis. The low stability of the $CO_2^{\delta-}$ species over $CeO_x/Cu(111)$ and $Cu/CeO_x/TiO_2(110)$ leads to MeOH synthesis rates that are significantly faster than those over traditional Cu/ZnO catalysts, as seen in Figure 2.

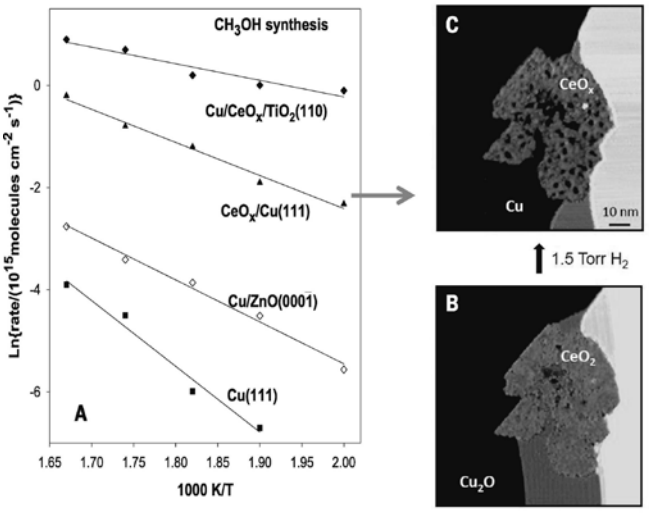

Figure 2. Arrhenius plot for methanol synthesis on Cu(111), a 0.2 ML of Cu on ZnO(0001), a Cu(111) surface covered 20% by ceria, and a 0.1 ML of Cu on a $TiO_2(110)$ surface pre-covered 15% with ceria (a). STM image of a $CeO_x/Cu(111)$ surface as prepared (b). *In-situ* STM image taken during exposure to 1.5 Torr of H_2 at 27 °C after 26 hours of reaction (c). (Reproduced from ref. 96 with permission from the American Association for the Advancement of Science.)

The study by Graciani et al. over $CeO_x/Cu(111)$ offers a different mechanism from the majority of researchers for MeOH synthesis from CO_2.[97] Most studies propose that the first step of MeOH synthesis is the direct hydrogenation of CO_2 through a formate intermediate, while Graciani et al. proposes

that the overall mechanism is RWGS followed by CO hydrogenation to MeOH. A recent study over Pd-Cu/SiO_2 also shows that CO produced through RWGS contributes to MeOH synthesis.[59]

Similar to the study of Graciani et al., DFT calculations over Mo_6S_8, a structural building block of MoS_2, show that MeOH synthesis proceeds through RWGS followed by CO hydrogenation to MeOH,[98] which is consistent with studies over CoMoS.[60] Investigations of Rh-based bimetallic catalysts indicate that CO is the intermediate,[61] with XPS measurements over Rh-Co/SiO_2 showing a surface enriched in Co; however, the more desirable surface is enriched in Rh, which correlates with CO stabilization and higher MeOH selectivity.[99] Observations from these studies indicates that the mechanism of MeOH synthesis from CO_2 is controversial, with researchers providing evidence for both formate and CO being the intermediates.

A recent study of low-pressure CH_3OH synthesis over Au/CeO_x/TiO_2 model catalysts also indicate that charge redistribution over metal particles may play a role.[100] The addition of CeO_x over Au/CeO_x/TiO_2 leads to increases in both CO_2 conversion and CH_3OH selectivity. AP-XPS measurements reveal that Au is partially negatively charged and CeO_x is in the Ce^{3+} state. The presence of adjacent negatively charged Au and Ce^{3+} sites enhances the adsorption strength of CO_2, leading to the higher CH_3OH yield.

Regardless of the exact nature of the intermediate, there is a necessity for more researchers to take advantage of DFT to identify potential descriptors that correlate with MeOH yield. By using the BEEF-vdW[101] functional, it has been shown that all of the relevant energy kinetics of MeOH synthesis can be mapped using one parameter, the oxygen adsorption energy (ΔE_O). Plotting TOF of CO_2 hydrogenation versus ΔE_O leads to a volcano relationship with Cu/ZnO and Ni-Ga at the peak. These two materials exhibit an optimal interaction with oxygen, resulting in stabilization of intermediates without poisoning the surface.[62] As more experimental results become available, future studies should continue to use DFT to develop descriptors to identify other novel and active materials for MeOH synthesis from CO_2 and H_2.

CO_2-FT for Alkane and Olefin Production

Another promising route is the direct production of hydrocarbons, including both alkanes and olefins, from direct Fischer-Tropsch with CO_2 and H_2 (CO_2-FT). Olefins are produced on the order of 200 Mt per year and result in 1.2 – 1.8 tons of CO_2 emitted per ton of olefin produced.[15] By manufacturing these products with a CO_2 feedstock, the net CO_2 emissions of the process will substantially decrease. However, designing active catalysts for CO_2-FT is difficult because they should be active for both RWGS and FT. Thermodynamics suggest that CO_2-FT becomes more favorable as higher chain compounds are formed because RWGS is slightly endothermic and the FT process is exothermic.[102, 103] Furthermore, high conversion of CO_2 can only be achieved if the FT step is fast enough to overcome the thermodynamic limitation of RWGS, which is the main challenge for CO_2-FT.[104] Other difficulties with designing catalysts for CO_2-FT are that (1) CO_2 is likely a poison for CO hydrogenation catalysts[15] and (2) water, an unavoidable byproduct during CO_2-FT, is a known poison that influences catalyst activity and product selectivity, as seen in Figure 3.[105]

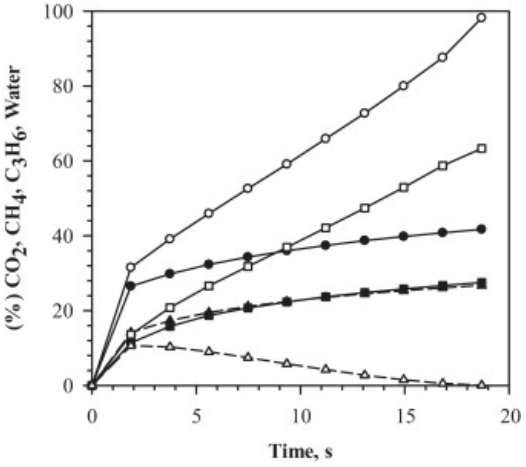

Figure 3. Comparison of model prediction for CO_2 conversion (○), C_3H_6 yield (□), and water (△) in catalytic tubular reactor with water removal, represented by hollow symbols and without water removal, represented by solid symbols. (Reproduced from ref. 104 with permission from Elsevier.)

The most commonly used metals in typical FT with syngas ($CO + H_2$) are Fe at higher temperatures and Co at lower temperatures. Generally, when comparing CO and CO_2 FT, CO conversion (up to 87%) is much higher than CO_2 conversion (up to 45%),[15] indicating that current FT catalysts are not adequate for CO_2-FT. Furthermore, in CO_2-FT, Co catalysts lead to high methane production and a deviation from the Anderson-Schultz-Flory (ASF) distribution.[106] This is further supported by a study over Co-based catalysts which shows that CO forms typical FT products, while CO_2 produces CH_4 over Co/SiO_2 and Co-Pt/γ-Al_2O_3.[107] Therefore, new and improved catalysts should be investigated to synthesize typical FT products with CO_2 as the carbon source.

Current research into CO_2-FT primarily focuses on Fe-based catalysts, which yield higher olefins than Co-based catalysts.[108, 109] Fe supported on γ-Al_2O_3 promotes C_2+ hydrocarbon formation, while Ni catalysts yield CH_4 as the primary product.[110] The active site of these Fe-based catalysts is under intense debate. Some studies indicate that an iron carbide phase is active,[111] while others show that the FeO phase is active and interacts strongly with the support.[112] CO_2 reduction into long-chain hydrocarbons is significantly improved with the addition of effective promoters, for example, K promoters in Fe catalysts help stabilize the iron carbide phase and adding boron (B) leads to light olefin formation.[113] One hypothesis is that K promotes CO_2 binding and hinders hydrogen adsorption,[114] which leads to suppressed methane formation and increases the olefin to alkane ratio.[103] Adding manganese (Mn) in a Fe/γ-Al_2O_3 catalyst also promotes long-chain olefin synthesis and suppresses methane formation.[109]

BNL-111844-2016-JA

PERSPECTIVE

Table 3. Summary of reaction conditions with conversion and selectivity to the primary CO_2-FT product, when available, for selected catalysts.

Catalyst	H_2:CO_2 Ratio	Temperature (°C)	Pressure (MPa)	Conversion (%)	Selectivity (%)
Fe-La-Cu-K/TiO_2[103]	3:1	300	1	27	C_5-C_{15} (40)
Fe-Ru-Zn-K/TiO_2[103]	3:1	300	1	27	C_5-C_{15} (37)
Fe-Zr-Cu-K/TiO_2[103]	3:1	300	1	25	C_5-C_{15} (30)
Co-Pt/Al_2O_3[106]	1:1	220	1.9	6.8	CH_4 (93.1), C_2-C_4 (6.8)
Fe/Al_2O_3[109]	3:1	290	1.4	18.2	C_2-C_5+ (34.9)
Mn-Fe/Al_2O_3[109]	3:1	290	1.4	37.7	C_2-C_5+ (55.3)
K-Mn-Fe/Al_2O_3[109]	3:1	290	1.4	41.4	C_2-C_5+ (62.4)
Fe/Al_2O_3[110]	3:1	300	1.1	12.1	C_2-C_7 (38)
Fe/K-OMS-2[111]	2:1	120 – 320	13.7	45	C_2-C_6 (68.7)
Fe-K/Al_2O_3-MgO[112]	3:1	300	1.01	27.5	C_2-C_5+ (58.5)
Fe-Co-K/Al_2O_3[114]	3:1	300	1.1	31	C_2+ (69)
Co/Al_2O_3[115]	6:1	260	0.1	2.5	N/A
Co/MgO[115]	6:1	260	0.1	2.0	N/A
Co/SiO_2[115]	6:1	260	0.1	1.5	N/A
Ni/SiO_2[116]	4:1	350	0.1	28.4	CH_4 (86.7)
Ni/$Ce_xZr_{1-x}O_2$[116, 117]	4:1	350	0.1	70.6	CH_4 (98.6)
Ni/CeO_2[118]	4:1	350	0.1	~90	CH_4 (~100)
Ru/γ-Al_2O_3[119]	4:1	150 – 325	0.1	N/A	CH_4 (~100)
Ru/TiO_2[120]	4:1	160	0.1	100	CH_4 (100)
Pd-Mg/SiO_2[121]	4:1	450	0.1	59.2	CH_4 (95.3)
Pd-Ni/SiO_2[121]	4:1	450	0.1	50.5	CH_4 (89.0)
Pd-Li/SiO_2[121]	4:1	450	0.1	42.6	CH_4 (88.5)

When comparing results from the Fe-based catalysts to those of Co and Ni, the CO_2 conversion over Fe materials is generally higher due to their increased RWGS activity. However, it is possible that the active phase in Co-based materials is difficult to stabilize under reaction conditions. *In-situ* X-ray absorption near edge spectroscopy (XANES) and XPS measurements of Co/TiO_2 show that the CoO phase is more active than Co metal for CO_2 hydrogenation and larger particles are more active because they are more easily oxidized.[122] Traditional FT Co-based catalysts show similar intermediates during CO_2 and CO hydrogenation according to FTIR measurements of a Co/γ-Al_2O_3 catalyst, suggesting that the hydrogenation pathway might be the same for both reactants. When CO_2 and CO are introduced together as feed, CO hydrogenation is primarily observed with CO_2 hydrogenation as a minor pathway because of competitive adsorption.[123]

The future direction of CO_2-FT should be focused on synthesizing catalysts that are highly active, selective and water-resistant in the range of 100 – 300 °C. It has been shown that catalysts synthesized with silica improve stability in water, with examples being HZSM-5 zeolite[124] and iron-based catalysts,[125] while the type of support material can prevent sintering of the active metallic phase to ensure catalytic stability.[109] Additionally, carbon composites synthesized through deposition of mesoporous carbon by impregnation of sugars[126] are promising materials as they improve activity by increasing metal dispersion and preventing leaching into aqueous reaction media. Because there are several different promising synthesis routes and metals for CO_2-FT, a facile means of rapidly screening new materials with DFT calculated descriptors should help develop a new generation of improved catalysts.

Another hydrogenation route, CO_2 methanation, is appropriate in certain geographical regions. Although natural gas supplies are abundant in the U.S., CO_2 methanation is an attractive energy storage route for many European nations where renewable energy is relatively abundant and CO_2 emissions are regulated.[127] Several catalysts have shown promise for CO_2 methanation, including Ni-Fe,[128] Rh/TiO_2,[129] Ni/CeO_2,[118] Ni/CeO_2-ZrO_2,[117] and Ru/γ-Al_2O_3.[119] Supported Ni-based catalysts are the most promising and well-studied systems for CO_2 methanation, while noble metal (e.g., Ru and Rh) based catalysts show better activity and stability at low temperatures.[120, 130] Ru/γ-Al_2O_3 is particularly interesting as the catalyst can be treated with cycles of CO_2 and H_2 and remains active after multiple reaction cycles. Another study has shown similar behavior for reduced Ru/CeO_2,[131] while high methane yield (100% at 160 °C) can be achieved on highly dispersed Ru nanoparticles supported on TiO_2.[120] Low

temperature (25 – 150 °C) CO_2 methanation over Rh/γ-Al_2O_3 has been reported,[130] while high temperature operation is required over Pd–Mg/SiO_2 (450 °C) [121] and Pd–Ni/CeO_2 (300 °C).[23]

Dual-functional materials that can both adsorb and hydrogenate CO_2 to CH_4 are very promising for commercial applications. By combining Ru/γ-Al_2O_3 with CaO, the catalyst can adsorb CO_2 from flue gas, then hydrogenate the adsorbed CO_2 to CH_4 when treated with pure H_2.[132] This type of dual-functional material shows significant promise for practical applications as it can be used directly in a flue gas stream, without the need to purify and transport CO_2.

Two primary mechanisms have been proposed for CO_2 methanation. In the first one, CO_2 undergoes C=O bond cleavage to form CO, which is subsequently converted into methane. Here, adsorbed surface carbon (C_{ads}) is considered to be a possible key intermediate.[133-135] The second mechanism proposes that CO_2 is first activated into carbonates, which are then hydrogenated into formate and subsequently hydrogenated into methoxy species. This mechanism suggests that weak basic sites are required for CO_2 adsorption, which is supported by the higher activity of Ni/CeO_2-ZrO_2 over Ni/SiO_2.[116] DRIFTS studies by Das et al. show that CO_2 adsorbs as carbonate species on Al_2O_3 and MgO supports with some formate, which is stabilized by the metal-support interface.[115]

Challenges and Opportunities for CO_2 Reduction

Controlling the selectivity of CO_2 conversion by H_2 requires thorough understanding of the thermodynamics, kinetics and key reaction intermediates of the aforementioned three pathways. CO_2-FT and MeOH synthesis are both exothermic processes, but RWGS is endothermic. Therefore, the temperature regime should be carefully chosen depending on the reaction of interest, as shown in Figure 4. Furthermore, for MeOH synthesis and CO_2-FT, higher reaction pressures can help drive the reaction forward. Clearly, low temperature operation would result in significant energy and economic benefits; however, CO_2-FT and MeOH synthesis are kinetically limited while RWGS is thermodynamic limited under these low-temperature conditions.

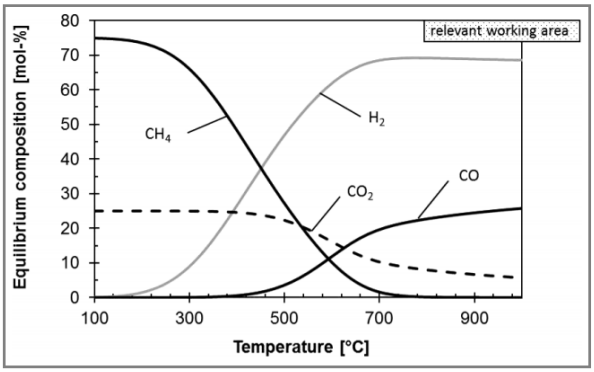

Figure 4. Thermodynamic equilibrium composition of the product gas of RWGS reaction at 0.1 MPa for a molar H_2:CO_2 inlet ratio of 3:1. (Reproduced from ref. 8 with permission from John Wiley and Sons.)

As outlined in detail above, the conversion of CO_2 to CO, CH_3OH, CH_4 and other hydrocarbons can occur via several possible routes. Figure 5 depicts some of the proposed pathways.[20, 88, 93, 97, 115, 116, 136] Along the formate pathways, the initial hydrogen transfer to CO_2 forms a formate (HCOO) species which undergoes series of hydrogenation and dissociation reactions to form CH_4 and CH_3OH. In contrast, along the RWGS and CO hydrogenation pathways, the initial hydrogenation of CO_2 forms a carboxylate (HOCO) species which undergoes dissociation reaction to form CO and OH. The CO intermediate then either desorbs or undergoes further hydrogenation reactions to form CH_3OH, CH_4 or other hydrocarbons.

For all three pathways of CO_2 reduction by H_2, there are significant challenges that should be addressed when designing active, selective and stable catalysts, as described below:

Stabilization of key intermediates

As described in each section for CO_2 reduction by H_2, the identification and stabilization of intermediates are critical for controlling the selectivity for each pathway. CO is perhaps the most important intermediate because catalysts with a stronger CO binding energy would favor MeOH[93] and hydrocarbon synthesis, while a weaker CO binding energy would favor RWGS. For MeOH synthesis, there is more work to be done in identifying the correct intermediate(s) and structure-property descriptors, but the latest research indicates that stabilization of CO is necessary for high MeOH yield. Identification of other descriptors with DFT calculations, such as oxygen adsorption energy,[62] adsorption configurations of CO_2 and key intermediates, and activation barriers for key reaction steps, should save a significant amount of time for catalyst screening and development.

Utilization of in-situ techniques

Parallel experiments on well-defined model surfaces are critical to support DFT calculations. However, most of the conventional UHV techniques are not very useful due to the weak adsorption strength of CO_2. Ambient pressure techniques, such as AP-XPS, AP-Temperature Programmed Reaction (AP-TPR), and infrared spectroscopy, should be utilized to determine the adsorption strength and configurations of CO_2 and key intermediates. Furthermore, *in-situ* techniques, such as environmental TEM and synchrotron-based XRD and X-ray absorption techniques, should be employed to characterize the electronic and structural properties of supported catalysts under reaction conditions.

Identification of low-cost catalysts

Significant reduction of CO_2 emissions requires large-scale processes and low-cost catalysts. These catalysts should also

exhibit reducible properties, which are an important feature of many catalysts for CO_2 reduction by H_2.[137] One promising material is Mo_2C, which is cost effective, reducible and has already been proven to reduce CO_2 by H_2.[39] However, Mo_2C is not ideal for CO_2-FT because it binds hydrocarbon intermediates relatively strongly, resulting in coke formation. Future efforts should focus on metal-modifications to attenuate the Mo_2C binding energy of intermediates, much like what is seen in a MeOH synthesis study with Cu-Mo_2C.[55]

Poisoning by Water

In all cases of CO_2 reduction by H_2, the production of large amounts of water is unavoidable, leading to catalyst poisoning through hydroxyl formation.[95] New water-tolerant catalysts should be identified that are stable under CO_2 reduction by H_2 conditions. Some promising materials are bimetallic particles encapsulated in porous SiO_2[138] and carbon shells.[139] Recent results by Qiao et al. show outstanding thermal stability and good recyclability for Pd and Pt particles encased in microporous Si shells[138] and PtCo has been proven to be active for CO_2 hydrogenation when encased in SiO_2 microspheres.[140] If this SiO_2 microsphere technology can be extended from precious metals to lower-cost materials, it could be possible to design highly active and stable catalysts which repel water.

Figure 5. *Reaction scheme for the conversion of CO_2 to CO, CH_3OH, CH_4 and other hydrocarbons.*

Development of CO_2-free H_2 sources

Currently, 95% of H_2 is produced from hydrocarbon based feedstocks (steam reforming of CH_4, coal gasification and partial oxidation of light oil residues), with CO_2 as a byproduct. A large-scale reduction of CO_2 requires sources of relatively inexpensive, renewable and CO_2-free H_2.[141] If the cost of renewable H_2 can be reduced to \$2.75 kg^{-1}, fuel from CO_2 becomes cost competitive with gasoline,[142] and the production of light olefins becomes economically viable.[143] Currently biomass conversion[144] and water electrolysis show promise for producing CO_2-free H_2. On a large-scale, the latter is likely the only suitable source of CO_2-free H_2 as it does not result in other byproducts except O_2.[137] Although recent studies have identified lower-cost electrocatalysts for hydrogen evolution in both acid[145] and alkaline[146] electrolytes, significant improvement in overall process cost is needed to produce enough H_2 for substantially reducing CO_2 emissions.

CO_2 Reduction by Alkanes

Alternatively, until CO_2-free H_2 can be produced on a large scale, light alkanes can be used to replace H_2 for CO_2 reduction. Researchers have attempted dry reforming of methane to produce synthesis gas, but high reaction temperatures (~700 °C) along with rapid deactivation of catalysts have prevented breakthroughs.[147] Dry reforming of ethane, however, becomes thermodynamically favorable about 100 °C lower than that of methane, making the process more feasible under milder conditions.[12] Furthermore, by reducing CO_2 with light alkanes, it might be possible to produce synthesis gas and olefins, both of which are valuable products.[148]

Comparison with Electrochemical Reduction

Although the current Perspective focuses on thermal catalysis, it should be pointed out that significant efforts are taking place in the

electrocatalytic reduction of CO_2, as summarized in recent reviews.[149, 150] One of the main advantages of electrocatalysis is that the hydrogen source for CO_2 reduction is from water instead from H_2 in thermal catalysis. Some of the current challenges in electrocatalysis include the relatively low Faradic efficiency for CO_2 conversion due to the high activity of the competing hydrogen evolution reaction (HER). Product separation might also present a challenge if low concentrations of oxygenate products, such as methanol and formic acid, are produced in water-based electrolytes. Opportunities in utilizing hybrid thermal-electrochemical approaches should be explored for CO_2 reduction.

Conclusions

In summary, several routes have been explored for CO_2 reduction by H_2. CO production through RWGS can be used in down-stream FT and MeOH synthesis, direct MeOH synthesis offers a liquid product with many industrial applications and finally, CO_2-FT produces olefins and alkanes that can be used directly as fuels or in the synthesis of plastics, surfactants, and detergents. Currently there is no preferred route for CO_2 reduction by H_2 because the specific application ultimately dictates which route is the most attractive. In any event, mitigation of atmospheric CO_2 is required on a large scale to prevent ocean acidification and climate change. Significant efforts must be put forth to both identify new catalysts and reduce the cost of CO_2-free H_2 to make CO_2 reduction by H_2 scientifically and economically viable.

Acknowledgements

The work was sponsored under Contract No. DE-FG02-13ER16381

References

1. T. R. Knutson and R. E. Tuleya, *J. Clim.*, 2004, **17**, 3477-3495.
2. J. Hansen, M. Sato, R. Ruedy, K. Lo, D. W. Lea and M. Medina-Elizade, *P. Natl. Acad. Sci. USA*, 2006, **103**, 14288-14293.
3. M. Aresta and A. Dibenedetto, *Dal. Trans.*, 2007, 2975-2992.
4. W. Wang, S. Wang, X. Ma and J. Gong, *Chem. Soc. Rev.*, 2011, **40**, 3703-3727.
5. G. Centi and S. Perathoner, *Catal. Today*, 2009, **148**, 191-205.
6. S. Perathoner and G. Centi, *ChemSusChem*, 2014, **7**, 1274-1282.
7. C. Song, *Catal. Today*, 2006, **115**, 2-32.
8. P. Kaiser, R. B. Unde, C. Kern and A. Jess, *Chem-Ing-Tech*, 2013, **85**, 489-499.
9. K. P. Kuhl, E. R. Cave, D. N. Abram and T. F. Jaramillo, *Ener. Environ. Sci.*, 2012, **5**, 7050-7059.
10. Q. Lu, J. Rosen, Y. Zhou, G. S. Hutchings, Y. C. Kimmel, J. G. Chen and F. Jiao, *Nat. Commun.*, 2014, **5**, 6.
11. T. Riedel, G. Schaub, K.-W. Jun and K.-W. Lee, *Ind. Eng. Chem. Res.*, 2001, **40**, 1355-1363.
12. Xu and J. A. Moulijn, *Energ. Fuel*, 1996, **10**, 305-325.
13. X.-M. Liu, G. Q. Lu, Z.-F. Yan and J. Beltramini, *Ind. Eng. Chem. Res.*, 2003, **42**, 6518-6530.
14. J. B. Hansen and P. E. H. Nielsen, *Journal*, 2008.
15. G. Centi and S. Perathoner, eds., *Green Carbon Dioxide: Advances in CO2 Utilization*, John Wiley & Sons, Hoboken, NJ, 2014.
16. B. W. Lu and K. Kawamoto, *Mater. Res. Bull.*, 2014, **53**, 70-78.
17. M. Gines, A. J. Marchi and C. R. Apesteguia, *Appl. Catal. A-Gen.*, 1997, **154**, 155-171.
18. S. Fujita, M. Usui and N. Takezawa, *J. Catal.*, 1992, **134**, 220-225.
19. J. Yoshihara and C. T. Campbell, *J. Catal.*, 1996, **161**, 776-782.
20. C.-S. Chen, W.-H. Cheng and S.-S. Lin, *Catal. Lett.*, 2000, **68**, 45-48.
21. R. Todorovic and R. J. Meyer, *Catal. Today*, 2011, **160**, 242-248.
22. W. C. Conner and J. L. Falconer, *Chem. Rev.*, 1995, **95**, 759-788.
23. M. D. Porosoff and J. G. Chen, *J. Catal.*, 2013, **301**, 30-37.
24. S. Alayoglu, S. K. Beaumont, F. Zheng, V. V. Pushkarev, H. M. Zheng, V. Iablokov, Z. Liu, J. H. Guo, N. Kruse and G. A. Somorjai, *Top, Catal,*, 2011, **54**, 778-785.
25. M. R. Gogate and R. J. Davis, *Catal. Comm.*, 2010, **11**, 901-906.
26. A. G. Kharaji, A. Shariati and M. A. Takassi, *Chin. J. Chem. Eng.*, 2013, **21**, 1007-1014.
27. A. G. Kharaji, A. Shariati and M. Ostadi, *J. Nanosci. Nanotechnol.*, 2014, **14**, 6841-6847.
28. Z. Cheng, B. J. Sherman and C. S. Lo, *J. Chem. Phys.*, 2013, **138**, 1-12.
29. A. Bueno-Lopez, K. Krishna and M. Makkee, *Appl. Catal. A-Gen.*, 2008, **342**, 144-149.
30. D. J. Pettigrew, D. L. Trimm and N. W. Cant, *Catal. Lett.*, 1994, **28**, 313-319.
31. Q. D. Sun, J. Y. Ye, C. J. Liu and Q. F. Ge, *Greenh. Gases*, 2014, **4**, 140-144.
32. B. Zhao, Y.-x. Pan and C.-j. Liu, *Catal. Today*, 2012, **194**, 60-64.
33. S. S. Kim, H. H. Lee and S. C. Hong, *Appl. Catal. A-Gen.*, 2012, **423–424**, 100-107.
34. C. S. Chen, W. H. Cheng and S. S. Lin, *Appl. Catal. A-Gen.*, 2003, **238**, 55-67.
35. Y. Liu and D. Liu, *Int. J. Hydrog. Energy*, 1999, **24**, 351-354.
36. C. S. Chen, W. H. Cheng and S. S. Lin, *Appl. Catal. A-Gen.*, 2004, **257**, 97-106.
37. K. K. Bando, K. Soga, K. Kunimori and H. Arakawa, *Appl. Catal. A-Gen.*, 1998, **175**, 67-81.
38. H. Kusama, K. K. Bando, K. Okabe and H. Arakawa, *Appl. Catal. A-Gen.*, 2001, **205**, 285-294.

39. M. D. Porosoff, X. Yang, J. A. Boscoboinik and J. G. Chen, *Angew. Chem. Int. Edit.*, 2014, **53**, 6705-6709.
40. W. Xu, P. Ramírez, D. Stacchiola, J. Brito and J. Rodriguez, *Catal. Lett.*, 2015, 1-9.
41. J. A. Rodriguez, J. Evans, L. Feria, A. B. Vidal, P. Liu, K. Nakamura and F. Illas, *J. Catal.*, 2013, **307**, 162-169.
42. R. B. Levy and M. Boudart, *Science*, 1973, **181**, 547-549.
43. S. Posada-Perez, F. Vines, P. J. Ramirez, A. B. Vidal, J. A. Rodriguez and F. Illas, *Phys. Chem. Chem. Phys.*, 2014, **16**, 14912-14921.
44. M. D. Porosoff, S. Kattel, W. Li, P. Liu and J. G. Chen, *Chem. Comm.*, 2015, **51**, 6988-6991.
45. O.-S. Joo, K.-D. Jung, I. Moon, A. Y. Rozovskii, G. I. Lin, S.-H. Han and S.-J. Uhm, *Ind. Eng. Chem. Res.*, 1999, **38**, 1808-1812.
46. S. Kuld, C. Conradsen, P. G. Moses, I. Chorkendorff and J. Sehested, *Angew. Chem. Int. Edit.*, 2014, **53**, 5941-5945.
47. M. Behrens, F. Studt, I. Kasatkin, S. Kühl, M. Hävecker, F. Abild-Pedersen, S. Zander, F. Girgsdies, P. Kurr, B.-L. Kniep, M. Tovar, R. W. Fischer, J. K. Nørskov and R. Schlögl, *Science*, 2012, **336**, 893-897.
48. A. Bansode and A. Urakawa, *J. Catal.*, 2014, **309**, 66-70.
49. L. Angelo, K. Kobl, L. M. M. Tejada, Y. Zimmermann, K. Parkhomenko and A. C. Roger, *C. R. Chim.*, 2015, **18**, 250-260.
50. W. J. Cai, P. R. de la Piscina, J. Toyir and N. Homs, *Catal. Today*, 2015, **242**, 193-199.
51. I. U. Din, M. S. Shaharun, D. Subbarao and A. Naeem, *J. Power Sources*, 2015, **274**, 619-628.
52. F. L. Liao, Y. Q. Huang, J. W. Ge, W. R. Zheng, K. Tedsree, P. Collier, X. L. Hong and S. C. Tsang, *Angew. Chem. Int. Edit.*, 2011, **50**, 2162-2165.
53. A. Bansode, B. Tidona, P. R. von Rohr and A. Urakawa, *Catal. Sci. Technol.*, 2013, **3**, 767-778.
54. Y. Q. Song, X. R. Liu, L. F. Xiao, W. Wu, J. W. Zhang and X. M. Song, *Catal. Lett.*, 2015, **145**, 1272-1280.
55. J.-L. Dubois, K. Sayama and H. Arakawa, *Chem. Lett.*, 1992, **21**, 5-8.
56. J. Xiao, D. Mao, X. Guo and J. Yu, *Appl. Surf. Sci.*, 2015, **338**, 146-153.
57. G. Bonura, M. Cordaro, C. Cannilla, F. Arena and F. Frusteri, *Appl. Catal. B-Environ.*, 2014, **152–153**, 152-161.
58. S. Kiatphuengporn, M. Chareonpanich and J. Limtrakul, *Chem. Eng. J.*, 2014, **240**, 527-553.
59. X. Jiang, N. Koizumi, X. W. Guo and C. S. Song, *Appl. Catal. B-Environ.*, 2015, **170**, 173-185.
60. D. L. S. Nieskens, D. Ferrari, Y. Liu and R. Kolonko Jr, *Catal. Comm.*, 2011, **14**, 111-113.
61. H. Kusama, K. Okabe, K. Sayama and H. Arakawa, *Catal. Today*, 1996, **28**, 261-266.
62. F. Studt, I. Sharafutdinov, F. Abild-Pedersen, C. F. Elkjær, J. S. Hummelshøj, S. Dahl, I. Chorkendorff and J. K. Nørskov, *Nat. Chem.*, 2014, **6**, 320-324.
63. H. Ahouari, A. Soualah, A. Le Valant, L. Pinard, P. Magnoux and Y. Pouilloux, *Reac. Kinet. Mech. Cat.*, 2013, **110**, 131-145.
64. S. Fujita, Y. Kanamori, A. M. Satriyo and N. Takezawa, *Catal. Today*, 1998, **45**, 241-244.
65. A. Le Valant, C. Comminges, C. Tisseraud, C. Canaff, L. Pinard and Y. Pouilloux, *J. Catal.*, 2015, **324**, 41-49.
66. H. Zhan, F. Li, C. Xin, N. Zhao, F. Xiao, W. Wei and Y. Sun, *Catal. Lett.*, 2015, **145**, 1177-1185.
67. J. Xiao, D. Mao, X. Guo and J. Yu, *Energ. Tech.*, 2015, **3**, 32-39.
68. H. Lei, R. Nie, G. Wu and Z. Hou, *Fuel*, 2015, **154**, 161-166.
69. Y. Hartadi, D. Widmann and R. J. Behm, *ChemSusChem*, 2015, **8**, 456-465.
70. G. Wang, L. Chen, Y. Sun, J. Wu, M. Fu and D. Ye, *RSC Adv.*, 2015, **5**, 45320-45330.
71. X.-L. Liang, J.-R. Xie and Z.-M. Liu, *Catal. Lett.*, 2015, **145**, 1138-1147.
72. J. Qu, X. Zhou, F. Xu, X.-Q. Gong and S. C. E. Tsang, *J. Phys. Chem. C*, 2014, **118**, 24452-24466.
73. H. Zhan, F. Li, P. Gao, N. Zhao, F. Xiao, W. Wei, L. Zhong and Y. Sun, *J. Power Sources*, 2014, **251**, 113-121.
74. P. Gao, F. Li, N. Zhao, F. Xiao, W. Wei, L. Zhong and Y. Sun, *Appl. Catal. A-Gen.*, 2013, **468**, 442-452.
75. R. Ladera, F. J. Perez-Alonso, J. M. Gonzalez-Carballo, M. Ojeda, S. Rojas and J. L. G. Fierro, *Appl. Catal. B-Environ.*, 2013, **142**, 241-248.
76. F. Arena, G. Mezzatesta, G. Zafarana, G. Trunfio, F. Frusteri and L. Spadaro, *J. Catal.*, 2013, **300**, 141-151.
77. X. Guo, D. Mao, G. Lu, S. Wang and G. Wu, *J. Mol. Catal. A-Chem.*, 2011, **345**, 60-68.
78. H. Kong, H.-Y. Li, G.-D. Lin and H.-B. Zhang, *Catal. Lett.*, 2011, **141**, 886-894.
79. L. Jia, J. Gao, W. Fang and Q. Li, *Catal. Comm.*, 2009, **10**, 2000-2003.
80. D. L. Chiavassa, J. Barrandeguy, A. L. Bonivardi and M. A. Baltanas, *Catal. Today*, 2008, **133**, 780-786.
81. J. Sloczynski, R. Grabowski, A. Kozlowska, P. Olszewski, J. Stoch, J. Skrzypek and M. Lachowska, *Appl. Catal. A-Gen.*, 2004, **278**, 11-23.
82. I. Melian-Cabrera, M. L. Granados and J. Fierro, *Catal. Lett.*, 2002, **79**, 165-170.
83. J. Toyir, P. R. de la Piscina, J. Fierro and N. Homs, *Appl. Catal. B-Environ.*, 2001, **34**, 255-266.
84. L. Z. Gao and C. T. Au, *J. Catal.*, 2000, **189**, 1-15.
85. J. Nakamura, J. A. Rodriguez and C. T. Campbell, *J. Phys. Cond. Mat.*, 1989, **1**, SB149.
86. A. B. Vidal, L. Feria, J. Evans, Y. Takahashi, P. Liu, K. Nakamura, F. Illas and J. A. Rodriguez, *J. Phys. Chem. Lett.*, 2012, **3**, 2275-2280.
87. J. Liu, J. Shi, D. He, Q. Zhang, X. Wu, Y. Liang and Q. Zhu, *Appl. Catal. A-Gen.*, 2001, **218**, 113-119.
88. E. L. Uzunova, N. Seriani and H. Mikosch, *Phys. Chem. Chem. Phys.*, 2015, **17**, 11088-11094.

89. J. Nakamura, I. Nakamura, T. Uchijima, T. Watanabe and T. Fujitani, in *Studies in Surface Science and Catalysis*, eds. W. N. D. E. I. Joe W. Hightower and T. B. Alexis, Elsevier, 1996, vol. Volume 101, pp. 1389-1399.
90. T. Fujitani, I. Nakamura, T. Uchijima and J. Nakamura, *Surf. Sci.*, 1997, **383**, 285-298.
91. Y. Yang, C. A. Mims, D. H. Mei, C. H. F. Peden and C. T. Campbell, *J. Catal.*, 2013, **298**, 10-17.
92. Y.-F. Zhao, Y. Yang, C. Mims, C. H. F. Peden, J. Li and D. Mei, *J. Catal.*, 2011, **281**, 199-211.
93. Y. Yang, J. Evans, J. A. Rodriguez, M. G. White and P. Liu, *Phys. Chem. Chem. Phys.*, 2010, **12**, 9909-9917.
94. Y. Yang, M. G. White and P. Liu, *J. Phys. Chem. C*, 2012, **116**, 248-256.
95. O. Martin and J. Perez-Ramirez, *Catal. Sci. Technol.*, 2013, **3**, 3343-3352.
96. J. Graciani, K. Mudiyanselage, F. Xu, A. E. Baber, J. Evans, S. D. Senanayake, D. J. Stacchiola, P. Liu, J. Hrbek, J. F. Sanz and J. A. Rodriguez, *Science*, 2014, **345**, 546-550.
97. M. Behrens, *Angew. Chem. Int. Edit.*, 2014, **53**, 12022-12024.
98. P. Liu, Y. Choi, Y. Yang and M. G. White, *J. Phys. Chem. A*, 2010, **114**, 3888-3895.
99. H. Kusama, K. Okabe and H. Arakawa, *Appl. Catal. A-Gen.*, 2001, **207**, 85-94.
100. X. Yang, S. Kattel, S. D. Senanayake, J. A. Boscoboinik, X. Nie, J. Graciani, J. A. Rodriguez, P. Liu, D. J. Stacchiola and J. G. Chen, *J. Am. Chem. Soc.*, 2015, **137**, 10104-10107.
101. F. Studt, F. Abild-Pedersen, J. Varley and J. Nørskov, *Catal. Lett.*, 2013, **143**, 71-73.
102. K. Müller, L. Mokrushina and W. Arlt, *Chem-Ing-Tech*, 2014, **86**, 497-503.
103. U. Rodemerck, M. Holeňa, E. Wagner, Q. Smejkal, A. Barkschat and M. Baerns, *ChemCatChem*, 2013, **5**, 1948-1955.
104. H. D. Willauer, R. Ananth, M. T. Olsen, D. M. Drab, D. R. Hardy and F. W. Williams, *J. CO2 Util.*, 2013, **3–4**, 56-64.
105. Y.-x. Pan, C.-j. Liu and Q. Ge, *J. Catal.*, 2010, **272**, 227-234.
106. R. W. Dorner, D. R. Hardy, F. W. Williams, B. H. Davis and H. D. Willauer, *Energ. Fuel*, 2009, **23**, 4190-4195.
107. Y. Q. Zhang, G. Jacobs, D. E. Sparks, M. E. Dry and B. H. Davis, *Catal. Today*, 2002, **71**, 411-418.
108. R. W. Dorner, D. R. Hardy, F. W. Williams and H. D. Willauer, *Ener. Environ. Sci.*, 2010, **3**, 884-890.
109. R. W. Dorner, D. R. Hardy, F. W. Williams and H. D. Willauer, *Appl. Catal. A-Gen.*, 2010, **373**, 112-121.
110. R. Satthawong, N. Koizumi, C. Song and P. Prasassarakich, *Top, Catal,*, 2014, **57**, 588-594.
111. B. Hu, S. Frueh, H. F. Garces, L. Zhang, M. Aindow, C. Brooks, E. Kreidler and S. L. Suib, *Appl. Catal. B-Environ.*, 2013, **132–133**, 54-61.
112. G. Kishan, M. W. Lee, S. S. Nam, M. J. Choi and K. W. Lee, *Catal. Lett.*, 1998, **56**, 215-219.
113. Z. You, W. Deng, Q. Zhang and Y. Wang, *Chin. J. Catal.*, 2013, **34**, 956-963.
114. R. Satthawong, N. Koizumi, C. S. Song and P. Prasassarakich, *Catal. Today*, 2015, **251**, 34-40.
115. T. Das and G. Deo, *J. Mol. Catal. A-Chem*, 2011, **350**, 75-82.
116. P. A. U. Aldana, F. Ocampo, K. Kobl, B. Louis, F. Thibault-Starzyk, M. Daturi, P. Bazin, S. Thomas and A. C. Roger, *Catal. Today*, 2013, **215**, 201-207.
117. F. Ocampo, B. Louis, L. Kiwi-Minsker and A.-C. Roger, *Appl. Catal. A-Gen.*, 2011, **392**, 36-44.
118. S. Tada, T. Shimizu, H. Kameyama, T. Haneda and R. Kikuchi, *Int. J. Hydrog. Energy*, 2012, **37**, 5527-5531.
119. C. Janke, M. S. Duyar, M. Hoskins and R. Farrauto, *Appl. Catal. B-Environ.*, 2014, **152**, 184-191.
120. T. Abe, M. Tanizawa, K. Watanabe and A. Taguchi, *Ener. Environ. Sci.*, 2009, **2**, 315-321.
121. J.-N. Park and E. W. McFarland, *J. Catal.*, 2009, **266**, 92-97.
122. G. Melaet, W. T. Ralston, C.-S. Li, S. Alayoglu, K. An, N. Musselwhite, B. Kalkan and G. A. Somorjai, *J. Am. Chem. Soc.*, 2014, **136**, 2260-2263.
123. C. G. Visconti, L. Lietti, E. Tronconi, P. Forzatti, R. Zennaro and E. Finocchio, *Appl. Catal. A-Gen.*, 2009, **355**, 61-68.
124. Y. Zhao, H. Wu, W. Tan, M. Zhang, M. Liu, C. Song, X. Wang and X. Guo, *Catal. Today*, 2010, **156**, 69-73.
125. T. Herranz, S. Rojas, F. J. Pérez-Alonso, M. Ojeda, P. Terreros and J. L. G. Fierro, *Appl. Catal. A-Gen.*, 2006, **308**, 19-30.
126. A. Jean-Marie, A. Griboval-Constant, A. Y. Khodakov and F. Diehl, *Catal. Today*, 2011, **171**, 180-185.
127. W. Davis and M. Martin, *J. Clean Prod.*, 2014, **80**, 252-261.
128. D. Pandey and G. Deo, *J. Mol. Catal. A-Chem.*, 2014, **382**, 23-30.
129. J. C. Matsubu, V. N. Yang and P. Christopher, *J. Am. Chem. Soc.*, 2015, **137**, 3076-3084.
130. M. Jacquemin, A. Beuls and P. Ruiz, *Catal. Today*, 2010, **157**, 462-466.
131. D. C. Upham, A. R. Derk, S. Sharma, H. Metiu and E. W. McFarland, *Catal. Sci. Technol.*, 2015, **5**, 1783-1791.
132. M. S. Duyar, M. A. A. Treviño and R. J. Farrauto, *Appl. Catal. B-Environ.*, 2015, **168–169**, 370-376.
133. D. E. Peebles, D. W. Goodman and J. M. White, *J. Phys. Chem.*, 1983, **87**, 4378-4387.
134. J. L. Falconer and A. E. Zagli, *J. Catal.*, 1980, **62**, 280-285.
135. G. D. Weatherbee and C. H. Bartholomew, *J. Catal.*, 1982, **77**, 460-472.
136. M. Ojeda, R. Nabar, A. U. Nilekar, A. Ishikawa, M. Mavrikakis and E. Iglesia, *J. Catal.*, 2010, **272**, 287-297.

137. E. V. Kondratenko, G. Mul, J. Baltrusaitis, G. O. Larrazabal and J. Perez-Ramirez, *Ener. Environ. Sci.*, 2013, **6**, 3112-3135.
138. Z.-A. Qiao, P. Zhang, S.-H. Chai, M. Chi, G. M. Veith, N. C. Gallego, M. Kidder and S. Dai, *J. Am. Chem. Soc.*, 2014, **136**, 11260-11263.
139. G.-H. Wang, J. Hilgert, F. H. Richter, F. Wang, H.-J. Bongard, B. Spliethoff, C. Weidenthaler and F. Schüth, *Nat. Mater.*, 2014, **13**, 293-300.
140. S. Takenaka, A. Hirata, E. Tanabe, H. Matsune and M. Kishida, *J. Catal.*, 2010, **274**, 228-238.
141. G. Centi, E. A. Quadrelli and S. Perathoner, *Ener. Environ. Sci.*, 2013, **6**, 1711-1731.
142. Q. Smejkal, U. Rodemerck, E. Wagner and M. Baerns, *Chem-Ing-Tech*, 2014, **86**, 679-686.
143. G. Centi, G. Iaquaniello and S. Perathoner, *ChemSusChem*, 2011, **4**, 1265-1273.
144. M. R. Stonor, T. E. Ferguson, J. G. Chen and A.-H. A. Park, *Ener. Environ. Sci.*, 2015, **8**, 1702-1706.
145. D. V. Esposito and J. G. Chen, *Ener. Environ. Sci.*, 2011, **4**, 3900-3912.
146. Q. Lu, G. S. Hutchings, W. Yu, Y. Zhou, R. V. Forest, R. Tao, J. Rosen, B. T. Yonemoto, Z. Cao, H. Zheng, J. Q. Xiao, F. Jiao and J. G. Chen, *Nat. Commun.*, 2015, **6**.
147. M. S. Fan, A. Z. Abdullah and S. Bhatia, *ChemCatChem*, 2009, **1**, 192-208.
148. M. D. Porosoff, M. Myint, S. Kattel, Z. Xie, E. Gomez, P. Liu and J. G. Chen, *Angew. Chem. Int. Edit.*, 2015, DOI: 10.1002/anie.201508128R201508121.
149. J. Qiao, Y. Liu, F. Hong and J. Zhang, *Chem. Soc. Rev.*, 2014, **43**, 631-675.
150. R. J. Lim, M. Xie, M. A. Sk, J.-M. Lee, A. Fisher, X. Wang and K. H. Lim, *Catal. Today*, 2014, **233**, 169-180.